

This is the accepted manuscript made available via CHORUS. The article has been published as:

Coulomb Mediated Hybridization of Excitons in Coupled Quantum Dots

P.-L. Ardelit, K. Gawarecki, K. Müller, A. M. Waeber, A. Bechtold, K. Oberhofer, J. M. Daniels, F. Klotz, M. Bichler, T. Kuhn, H. J. Krenner, P. Machnikowski, and J. J. Finley

Phys. Rev. Lett. **116**, 077401 — Published 19 February 2016

DOI: [10.1103/PhysRevLett.116.077401](https://doi.org/10.1103/PhysRevLett.116.077401)

Coulomb mediated hybridization of excitons in coupled quantum dots

P.-L. Ardel, ^{1,2} K. Gawarecki, ³ K. Müller, ^{1,4} A. M. Waeber, ¹ A. Bechtold, ¹ K. Oberhofer, ¹ J. M. Daniels, ⁵ F. Klotz, ¹ M. Bichler, ¹ T. Kuhn, ⁵ H.J. Krenner, ^{6,2} P. Machnikowski, ³ and J.J. Finley ^{1,2}

¹Walter Schottky Institut and Physik-Department,

Technische Universität München, Am Coulombwall 4, 85748 Garching, Germany

²Nanosystems Initiative Munich (NIM), Schellingstr. 4, 80339 München, Germany

³Department of Theoretical Physics, *Faculty of Fundamental Problems of Technology*,
Wrocław University of Technology, 50-370 Wrocław, Poland

⁴E.L.Ginzton Laboratory, Stanford University, Stanford, CA 94305, USA

⁵Institut für Festkörpertheorie, Westfälische Wilhelms-Universität Münster,
Wilhelm-Klemm-Strasse 10, 48149 Münster, Germany

⁶Lehrstuhl für Experimentalphysik 1 and Augsburg Centre for Innovative Technologies (ACIT),
Universität Augsburg, Universitätsstr. 1, 86159 Augsburg, Germany

(Dated: January 28, 2016)

We report Coulomb mediated hybridization of excitonic states in optically active InGaAs quantum dot molecules. By probing the optical response of an individual quantum dot molecule as a function of the static electric field applied along the molecular axis, we observe unexpected avoided level crossings that do not arise from the dominant single particle tunnel coupling. We identify a new few-particle coupling mechanism stemming from Coulomb interactions between different neutral exciton states. Such Coulomb resonances hybridize the exciton wave function over four different electron and hole single-particle orbitals. Comparisons of experimental observations with microscopic 8-band $k \cdot p$ calculations taking into account a realistic quantum dot geometry show good agreement and reveal that the Coulomb resonances arise from broken symmetry in the artificial semiconductor molecule.

Understanding and controlling the fundamental interactions that couple discrete quantum states lies at the very heart of applied quantum science. For example, couplings between distinct physical subsystems mediated by the Coulomb interaction can be used to entangle qubits electrostatically [1], to build single-photon transistors on the basis of Förster resonances [2] or to control resonant energy transfer [3]. Strong tunnel couplings between proximal quantum dots have been shown to facilitate electrical and optical spin-qubit operations [4, 5] while long range magnetic dipolar interactions have been exploited for prototype quantum registers [6]. Thus the nature of quantum couplings has been under extensive investigation for many prototypical quantum systems. Examples include naturally occurring atoms [3, 7, 8] and defect centers [9, 10] as well as artificial atoms and molecules [11–13]. Due to advanced nanostructure fabrication techniques [14, 15] and efficient coupling to light [16, 17], artificial semiconductor molecules consisting of pairs of quantum dots (QDs) have emerged as ideal prototypical solid-state systems to investigate and electrically control interactions between proximal quantum systems [11, 12].

By embedding a QD-molecule into the intrinsic region of a diode structure, exciton states in the different QDs can be tuned into and out of resonance by controlling the electric field along the growth direction [11, 12]. The fundamental signatures of quantum couplings are avoided level crossings in the electronic energy level structure of a QD-molecule as single particle states are tuned in and out of resonance [18]. The importance of Coulomb inter-

actions has been pointed out for the form and position of resonances in QD-molecule systems [19–21]. However, single particle tunneling that either hybridizes single electrons or holes remains the dominant coupling mechanism in these cases. This has been extensively studied for charge neutral as well as charged states and between similar orbitals as well as different orbitals [11–13, 22–25]. While all these couplings naturally emerge in a single particle picture, most recently another resonant coupling mechanism with an inherently two-particle nature has been predicted theoretically. This mechanism entirely relies on the Coulomb mediated interaction between two different exciton states [26]. In strong contrast to single-particle quantum couplings, such few-particle couplings have not yet been observed in QD-molecules.

In this letter, we apply complementary optical techniques to probe the excitonic energy level structure of an individual QD-molecule as a function of an externally applied electric field. We resolve a series of avoided energy level crossings that involve four different single particle orbital states, which cannot be explained by single-particle resonant tunneling. This novel few-particle coupling mechanism is shown to result from the Coulomb interaction alone, leading to a hybridization of both the electron and the heavy hole component of the neutral exciton [26]. Simulations of the energy structure using an 8-band $k \cdot p$ model and a realistic QD-molecule geometry that breaks the cylindrical symmetry are in good agreement with the measurements. They reveal the crucial role of broken symmetries for the emergence of the investigated few-particle couplings.

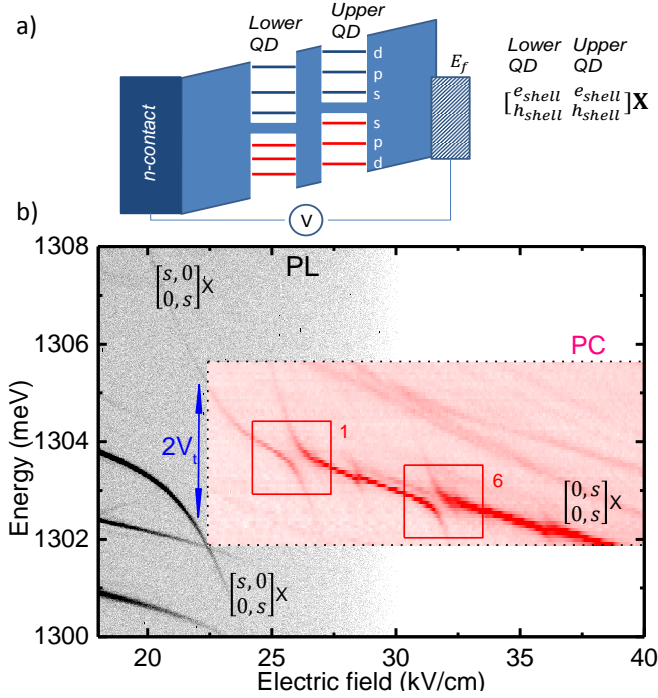


FIG. 1. (a) Schematic band structure diagram of a QD-molecule embedded in a Schottky diode with s -, p - and d -like orbitals of the lateral confinement, respectively. (b) Electric field dependent PL (grey) and PC (red) spectra. Avoided level crossing of the direct exciton $[0,s]X$ are marked by the blue arrow (tunneling) and red boxes.

The schematic band-structure of the QD-molecule is illustrated in Figure 1a. It consists of a vertically stacked pair of self-assembled InGaAs QDs that are separated by a 10 nm thick GaAs spacer. The QDs are embedded within the intrinsic region of a GaAs Schottky photodiode [11] to facilitate the application of internal electric fields F along the growth direction by tuning a gate potential V . Since electrons and holes can occupy a number of single-particle states in either the upper or lower dot of the molecule, we introduce the notation $[e_l, e_u, h_l, h_u]X$ to describe the exciton states in the system in Fig. 1a. Hereby, e_l, e_u, h_l and h_u denote the dominant orbital character of the single particle state involved as given by the in-plane symmetry (s, p, d) with the indices u and l representing the upper and lower dot respectively. For example $[0,s]X$ corresponds to a direct neutral exciton where an electron-hole pair is present in the upper dot of the QD-molecule with both single particles occupying the energetically lowest s -orbital. Similarly, $[s,0]X$ would correspond to a spatially indirect neutral exciton [11, 22].

In the grey scale part of Fig. 1b we present the photoluminescence (PL) intensity obtained from a single QD-molecule as a function of the applied electric field F at $T = 4.2$ K (greyscale). A pronounced avoided level crossing is observed for an electric field of $F = 21.8$ kV/cm with a splitting of $2V_t$. The underlying coupling of

strength V_t is well-known to arise from resonant tunneling of the direct exciton state $[0,s]X$ to the indirect exciton state $[s,0]X$ [11, 23]. For indirect excitons the electron e and hole h are separated in the upper and lower QD. Thereby, the indirect exciton transition $[s,0]X$ can be tuned into resonance with $[0,s]X$ by applying an electric field (due to its larger intrinsic dipole). When in resonance, the two states couple by single-particle tunneling of the electron between s -orbitals $[0,s]X \leftrightarrow [s,0]X$ leading to the avoided level crossing observed at $F = 21.8$ kV/cm in Fig. 1b [11, 22, 23].

By further increasing F , the PL intensity is quenched due to tunneling of the charge carriers out of the molecule, enabling photocurrent (PC) measurements [27]. Such measurements are presented in Fig. 1b (red scale), obtained by scanning a laser over the spectral window between 1302 meV and 1306 meV. They reveal a series of unexpected avoided level crossings for the $[0,s]X$ exciton state with splittings of $2V_t = 0.15 - 0.6$ meV. The most prominent ones are marked on Fig. 1b. Since the resonance observed at $F = 21.8$ kV/cm results from coupling of the direct exciton $[0,s]X$ to the indirect exciton $[s,0]X$ with the lowest orbital energy, we expect the couplings of $[0,s]X$ observed at higher electric field to result from coupling to energetically excited indirect excitons.

In order to identify the orbital character of the excitons involved in the avoided level crossings, we map out the energy level structure of the first few excited states of the direct exciton $[0,s]X$ by combining PL and PC measurements with field dependent photoluminescence excitation (PLE) spectroscopy [23]. This extends the energy level structure in Fig. 1b to higher energies and lower electric field. The results are presented in Fig. 2. At $F \sim 21.8$ kV/cm we observe a pair of avoided level crossings with a coupling strength of $\sim V_t$ (box 4) in the excited states (black triangles). The occurrence of avoided level crossings for the excited states $[0,s]X$ at a similar electric field and with comparable coupling strength to s - s tunnel coupling ($[s,0]X \leftrightarrow [0,s]X$) is well-known: as shown in Ref. [23], the avoided energy level crossings observed in the PL and the PLE around $F \sim 21.8$ kV/cm (box 3 and 4 on Fig. 2) arise from the same single-particle s - s orbital resonant tunneling of the electron. However, they differ in that the hole resides in the p -orbital of the upper dot (4) instead of the s -orbital (3). In both cases, the electron wave function is hybridized over the upper and lower QD by resonant tunnel coupling (inset 3 and 4 on Fig. 2).

In order to quantitatively analyze the coupling strengths, we use a phenomenological model [28] to fit the field-dependent exciton energies using the quantum confined Stark effect (QCSE) [29]. Here, the observed couplings between the different states with strengths V_n are introduced as off-diagonal elements in the Hamiltonian and are fitted to the data. The resulting eigenstates

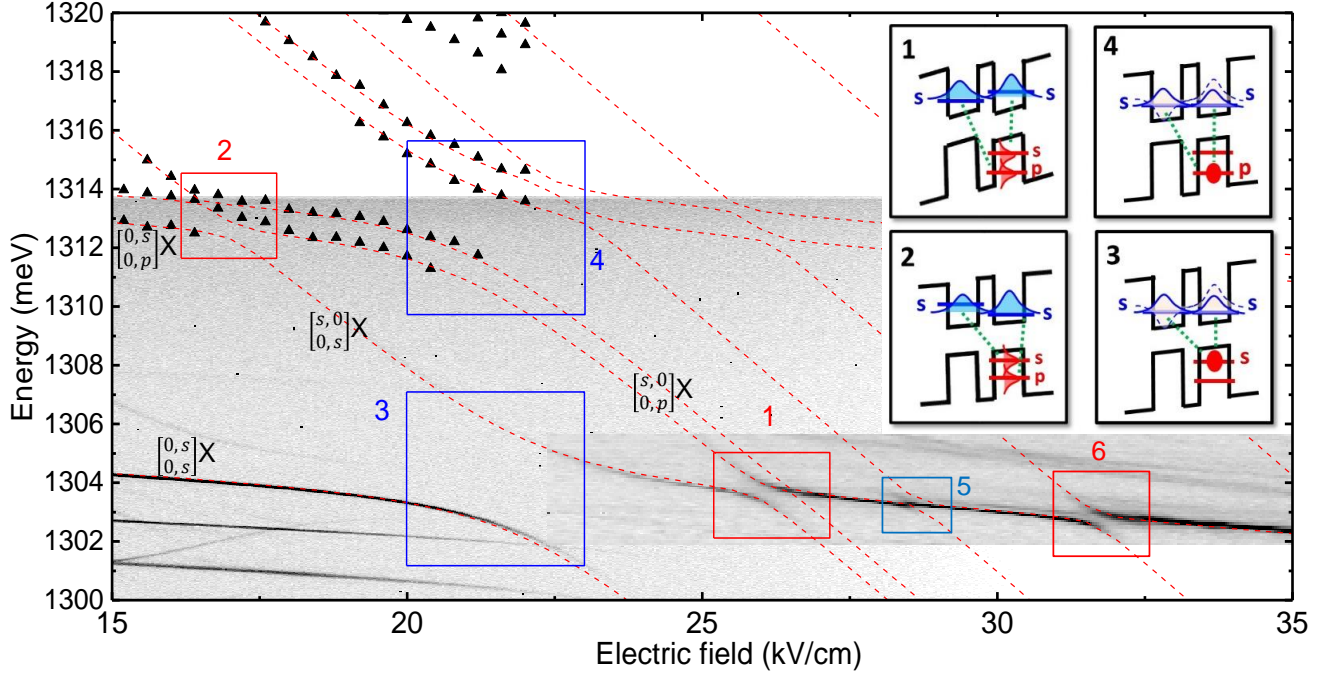


FIG. 2. Electronic energy level structure of a single QD-molecule mapped out by combining field-dependent PL, PC and PLE (black triangles) spectra. Fits to the levels based on the QCSE are presented as red lines. Avoided level crossing resulting from Coulomb resonances (resonant tunneling) are highlighted by red (blue) rectangles and illustrated in the inset.

are plotted as dashed red lines in Fig.2 producing very good overall agreement with the experimental PL and PLE results.

Having identified the excited indirect excitons $[s, 0]X$ and $[0, p_2]X$ from the resonant tunnel coupling $[0, p_1]X \Leftrightarrow [s, 0]X$ (box 4 in Fig.2), we trace them to lower energies where they would become resonant with the direct exciton $[0, s]X$ at $F_1 = 26.0$ kV/cm and $F_2 = 26.5$ kV/cm, respectively. Strikingly, as highlighted by the red box 1 on Fig.2, we observe an avoided level crossing of coupling strength $2V_{C(p_1)} = 0.6$ meV for the $[0, s]X \Leftrightarrow [s, 0]X$ resonance. We emphasize here, that in contrast to the case $[0, s]X \Leftrightarrow [s, 0]X$ at $F \sim 21.8$ kV/cm, the avoided level crossings $[0, s]X \Leftrightarrow [s, 0]X$ cannot arise from a single-particle coupling such as resonant tunneling since four *different* single particle orbitals are involved (see Fig.2 inset 1 and 2).

To confirm the universality of resonant couplings between direct and indirect excitons involving four different orbitals, we trace the direct excited states $[0, p_1]X$ and $[0, p_2]X$ in PLE spectroscopy to lower electric fields. At the point where they become resonant with $[s, 0]X$ at $F = 16.4$ kV/cm (see box 2 in Fig.2) a weak avoided level crossings is observed. Finally, to further support our findings, we performed the same measurements on a second QD-molecule resolving the same structure of avoided level crossings between excitonic states that cannot be coupled by resonant tunneling [29].

However, in contrast to single particle resonant tunneling, Coulomb mediated few-particle interactions are able to couple excitonic states constructed from four different single particle orbitals (inset on Fig. 2). At these resonances both the electron and hole component of the exciton are hybridized over two single particle orbitals. Such resonances correspond to off-diagonal Coulomb terms that couple direct and indirect exciton states and depend only on the mesoscopic carrier distribution described in terms of the envelope function [26]. While this kind of coupling is universal, it is governed by symmetry-related selection rules. Since the Coulomb interaction conserves angular momentum, exciton states with different axial projections of the angular momentum M have zero coupling strength assuming perfect symmetry and neglecting higher order spin-orbit interactions (the Dresselhaus terms). However, breaking the symmetry by introducing ellipticity of the QDs or a lateral displacement of the two QDs relative to each other rapidly increases the coupling strengths V_C among states with different angular momenta $\Delta M = \pm 2$ and $\Delta M = \pm 1$, respectively [26]. Notably, while the coupling strengths of the resonant tunneling couplings V_t are similar for both molecules, the coupling strengths of the Coulomb resonances V_C vary significantly more indicating a strong dependence on the individual morphology of each QD-molecule [29].

To investigate the emergence of Coulomb resonances, we performed detailed modeling using 8-band $k \cdot p$ theory and a configuration interaction approach. In our

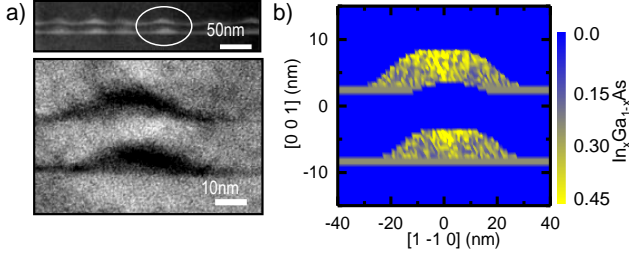


FIG. 3. (a) TEM-image of a QD-molecule. (b) Geometry used to model the QD-molecule resulting in the electronic structure presented in Fig.4.

modeling, we have included generic morphological properties of the QD system documented in the literature [30, 31]. This has allowed us to quantitatively reproduce the sample-invariant features of the spectrum, while the predicted characteristics of those spectral features that vary from sample to sample quantitatively fall in the range of observed values. In particular, good quantitative agreement between the numerical and experimental results can be obtained only if the asymmetry of the QD-molecule system and compositional inhomogeneity are included in the model. To this end, we use a QD-molecule geometry where the height and the lateral size are consistent with TEM [30] images of nominally identical QD-molecules as presented in Fig. 3a. For comparison, the modeled geometry is presented in Fig. 3b. Notably, the shape of the upper QD is perturbed by the presence of the strain field of the lower QD through the GaAs barrier [30]. In the modeled geometry, we include this perturbation induced by the lower QD by tilting up the upper QD (in the dot center) from the bottom of the wetting layer. Finally, we break the axial symmetry of the system by inducing a relative displacement of the QD centers in $(1\bar{1}0)$ direction [31]. The typically non-uniform $\text{In}_x\text{Ga}_{1-x}\text{As}$ composition in the QDs is accounted for by using a trumpet shape [32, 33] of the In-content with a maximum of $x = 0.43$ in the QDs and a homogeneous composition of $\text{In}_{0.25}\text{Ga}_{0.75}\text{As}$ in both wetting layers [29].

To include the effects of the strain on the band structure [34] originating from the $\text{In}_x\text{Ga}_{1-x}\text{As}/\text{GaAs}$ lattice mismatch, we calculate the strain tensor elements for the QD-molecule within the continuous elasticity approach by minimizing the elastic energy [35]. Due to the zinc-blende structure of the $\text{In}_x\text{Ga}_{1-x}\text{As}$ crystal, the shear strain induces a piezoelectric field that we take into account up to second order in polarization [36, 37] using the parameters from Ref. 38. The electron and hole orbital states of the QD-molecule are calculated using 8-band $k \cdot p$ theory as described in detail in Ref. 39. Finally, we calculate the exciton states using the configuration interaction approach [29].

The results of our calculations are presented in Fig. 4 which shows the energy level structure of the ener-

getically lowest neutral exciton transitions. In quantitative agreement with the experimentally observed coupling ($2V_t = 3.3 \text{ meV}$ in Fig. 2), we obtain avoided level crossings with $2V_{t(s)} = 3.05 \text{ meV}$ and $2V_{t(p_1/p_2)} = 3.08 \text{ meV}$ (3.0 meV) for resonant s-s orbital tunneling where the hole resides in the s-orbital $[\frac{0}{0,s}]X \Leftrightarrow [\frac{s}{0,s}]X$ (box 3 in Fig. 4) and $p_{1(2)}$ -orbital $[\frac{0}{0,p}]X \Leftrightarrow [\frac{s}{0,p}]X$ (box 4 in Fig. 4), respectively.

In our modeling, the angular momentum conservation of the Coulomb resonances is lifted by the lateral displacement of the QDs. The axial symmetry breaking leads to a significant s-p mixing of the electron states [39] and thus to an avoided level crossing at the s-p orbital electron tunneling resonance $[\frac{p}{0,s}]X \Leftrightarrow [\frac{s}{0,s}]X$. We observe this tunneling resonance in the calculated electronic spectrum (box 5 in Fig.4) with a somewhat smaller coupling strength than in the experiment (Fig.2). The resonance with the other p-state remains very weak as the electron wave function is oriented perpendicular to the displacement [39]. Most importantly, the numerical simulation reproduces the avoided level crossings due to few-particle couplings that are mediated by the Coulomb interaction: the resonances between the exciton states $[\frac{s}{0,p_{1(2)}}]X \Leftrightarrow [\frac{0}{0,s}]X$ and the exciton states $[\frac{s}{0,s}]X \Leftrightarrow [\frac{0}{0,p_{1(2)}}]X$ are calculated with a coupling strength of up to $\sim 0.23 \text{ meV}$ and are presented in the insets of Fig.4. The coupling strengths V_C of the Coulomb resonances in the numerical calculation are found within the range of values observed for the two QD-molecules (see Fig.2 and [29]). The variance of the coupling strengths V_C may be due to the particular sample-dependent asymmetries that may arise from additional spin-orbit couplings [26] or emerge from atomistic structure beyond the present model [40, 41].

Finally, in the numerically calculated and experimentally recorded energy level structure we resolve a Coulomb resonance where the hole resides in one of the d-orbitals $[\frac{s}{0,d}]X \Leftrightarrow [\frac{0}{0,s}]X$ (box 6 in Fig.4 and Fig.2). The assignment of the avoided level crossing to a Coulomb resonance is supported by additional PLE spectroscopy [29]. Overall, the comparison of the experimental and theoretical results confirms the proposed assignment of the avoided level crossings to stem from Coulomb mediated few-particle interactions and reveals the essential role of morphological features underlying the observed resonances.

In conclusion, we presented the direct observation of a novel, electrically-tunable few-particle coupling mechanism in QD-molecules: Coulomb resonances that involve four different single-particle orbitals and hybridize both the electron and hole component of the exciton. Numerical calculations using 8-band $k \cdot p$ theory with a realistic QD geometry are in good agreement with the experimental results. Ultimately, our results demonstrate how symmetry breaking in QD-molecules leads to the formation

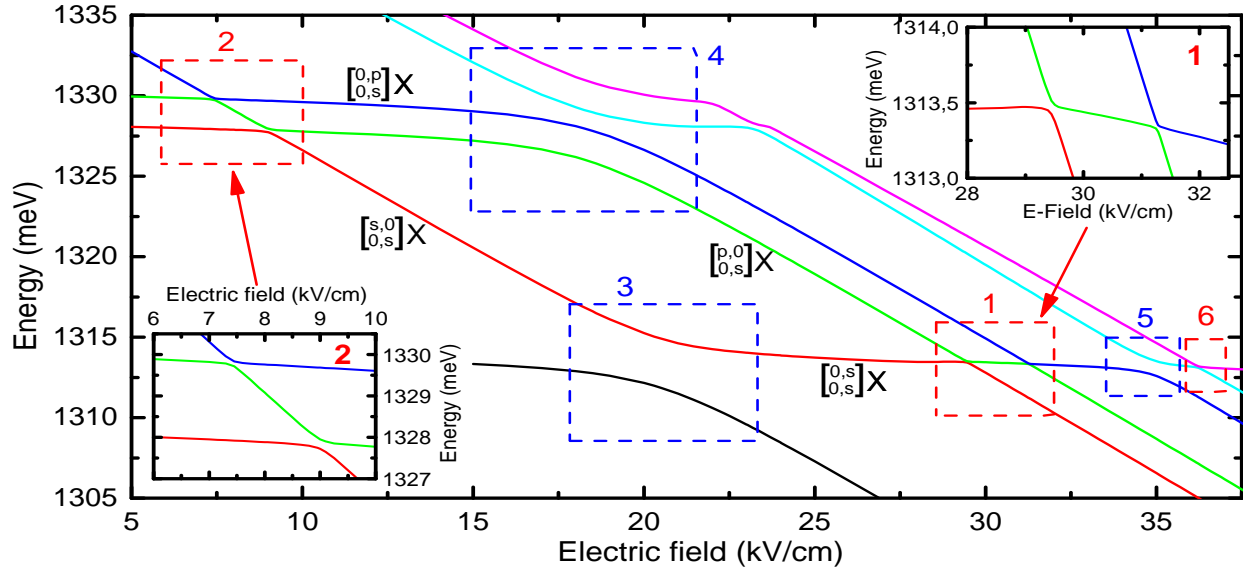


FIG. 4. Numerically calculated energy level structure using 8-band $k \cdot p$ theory and the QD-molecule geometry presented in Fig.3. Avoided level crossings resulting from few-particle Coulomb coupling (resonant tunneling) are highlighted in red (blue). The color coding and numbering of the avoided level crossings correspond to the coding in Fig.2.

of novel few-particle couplings.

While the experimentally convenient electrical control of the few-particle interactions makes them an interesting candidate for the realization of few-particle qubits, we suggest to use the Coulomb resonances as a sensor for the complex single-particle spectrum of the heavy holes in QDs [42]. As the Coulomb resonances map different hole states to spectral resonances of the optically active neutral exciton, for example tracking of the Coulomb resonances in magneto-optical measurements seems suitable to map out the Fock-Darwin spectra of heavy hole states in artificial atoms.

P.L.A., K.M., A.M.W., A.B., K.O., F.K., H.J.K. and J.J.F. gratefully acknowledge financial support from the DFG via SFB-631, the Nanosystems Initiative Munich and the EU via ITN S³ Nano. H.J.K. acknowledges support from the Emmy Noether Program and K.M. from the Alexander von Humboldt foundation as well as the ARO (grant W911NF-13-1-0309). K.G. acknowledges support by the Grant No. 2012/05/N/ST3/03079 from the Polish National Science Centre (Narodowe Centrum Nauki).

[1] M. D. Shulman, O. E. Dial, S. P. Harvey, H. Bluhm, V. Umansky, and A. Yacoby, *Science* **336**, 202 (2012).
 [2] D. Tiarks, S. Baur, K. Schneider, S. Dürr, and G. Rempe, *Phys. Rev. Lett.* **113**, 053602 (2014).
 [3] S. Ravets, H. Labuhn, D. Barredo, L. Béguin, T. Lahaye, and A. Browaeys, *Nat. Phys.* **10**, 914 (2014).

[4] A. Grelich, S. G. Carter, D. Kim, A. S. Bracker, and D. Gammon, *Nat. Phot.* **5**, 702 (2011).
 [5] J. R. Petta, A. C. Johnson, J. M. Taylor, E. A. Laird, A. Yacoby, M. D. Lukin, C. M. Marcus, M. P. Hanson, and A. C. Gossard, *Science* **309**, 2180 (2005).
 [6] P. Neumann, R. Kolesov, B. Naydenov, J. Beck, F. Rempp, M. Steiner, V. Jacques, G. Balasubramanian, M. L. Markham, D. J. Twitchen, S. Pezzagna, J. Meijer, J. Twamley, F. Jelezko, and J. Wrachtrup, *Nat. Phys.* **6**, 249 (2010).
 [7] W. R. Anderson, J. R. Veale, and T. F. Gallagher, *Phys. Rev. Lett.* **80**, 249 (1998).
 [8] C. S. E. Van Ditzhuijzen, A. F. Koenderink, J. V. Hernández, F. Robicheaux, L. D. Noordam, and H. B. L. Van Den Heuvel, *Phys. Rev. Lett.* **100**, 243201 (2008).
 [9] M. Veldhorst, C. H. Yang, J. C. C. Hwang, W. Huang, J. P. Dehollain, J. T. Muhonen, S. Simmons, A. Laucht, F. E. Hudson, K. M. Itoh, A. Morello, and A. S. Dzurak, *Nature* **526**, 410 (2015).
 [10] R. Kalra, A. Laucht, C. D. Hill, and A. Morello, *Phys. Rev. X* **4**, 021044 (2014).
 [11] H. J. Krenner, M. Sabathil, E. C. Clark, A. Kress, D. Schuh, M. Bichler, G. Abstreiter, and J. J. Finley, *Phys. Rev. Lett.* **94**, 057402 (2005).
 [12] E. A. Stinaff, M. Scheibner, A. S. Bracker, I. V. Ponomarev, V. L. Korenev, M. E. Ware, M. F. Doty, T. L. Reinecke, and D. Gammon, *Science* **311**, 636 (2006).
 [13] M. Scheibner, M. Yakes, A. S. Bracker, I. V. Ponomarev, M. F. Doty, C. S. Hellberg, L. J. Whitman, T. L. Reinecke, and D. Gammon, *Nat. Phys.* **4**, 291 (2008).
 [14] A. Faraon, I. Fushman, D. Englund, N. Stoltz, P. Petroff, and J. Vučković, *Nat. Phys.* **4**, 859 (2008).
 [15] A. K. Nowak, S. L. Portalupi, V. Giesz, O. Gazzano, C. Dal Savio, P. F. Braun, K. Karrai, C. Arnold, L. Lanco, I. Sagnes, A. Lemaitre, and P. Senellart, *Nat. Commun.* **5** (2014).

- [16] O. Gazzano, S. M. de Vasconcellos, C. Arnold, A. Nowak, E. Galopin, I. Sagnes, L. Lanco, A. Lemaître, and P. Senellart, *Nat. Commun.* **4**, 1425 (2013).
- [17] C. Arnold, J. Demory, V. Loo, A. Lemaître, I. Sagnes, M. Glazov, O. Krebs, P. Voisin, P. Senellart, and L. Lanco, *Nat. Commun.* **6** (2015).
- [18] W. Sheng and J. P. Leburton, *Phys. Rev. Lett.* **88**, 167401 (2002).
- [19] B. Szafran, T. Chwiej, F. M. Peeters, S. Bednarek, J. Adamowski, and B. Partoens, *Phys. Rev. B* **71**, 205316 (2005).
- [20] B. Szafran, F. M. Peeters, and S. Bednarek, *Phys. Rev. B* **75**, 115303 (2007).
- [21] B. Szafran, *Acta Physica Polonica* **A**, 1013 (2008).
- [22] H. J. Krenner, E. C. Clark, T. Nakaoka, M. Bichler, C. Scheurer, G. Abstreiter, and J. J. Finley, *Phys. Rev. Lett.* **97**, 076403 (2006).
- [23] K. Müller, G. Reithmaier, E. C. Clark, V. Jovanov, M. Bichler, H. J. Krenner, M. Betz, G. Abstreiter, and J. J. Finley, *Phys. Rev. B* **84**, 081302 (2011).
- [24] K. Müller, A. Bechtold, C. Ruppert, M. Zecherle, G. Reithmaier, M. Bichler, H. J. Krenner, G. Abstreiter, A. W. Holleitner, J. M. Villas-Boas, M. Betz, and J. J. Finley, *Phys. Rev. Lett.* **108**, 197402 (2012).
- [25] A. S. Bracker, M. Scheibner, M. F. Doty, E. A. Stinaff, I. V. Ponomarev, J. C. Kim, L. J. Whitman, T. L. Reinicke, and D. Gammon, *Appl. Phys. Lett.* **89**, 233110 (2006).
- [26] J. M. Daniels, P. Machnikowski, and T. Kuhn, *Phys. Rev. B* **88**, 205307 (2013).
- [27] F. Findeis, M. Baier, E. Beham, A. Zrenner, and G. Abstreiter, *Appl. Phys. Lett.* **78**, 2958 (2001).
- [28] R. J. Warburton, B. T. Miller, C. S. Dürr, C. Bödefeld, K. Karrai, J. P. Kotthaus, G. Medeiros-Ribeiro, P. M. Petroff, and S. Huant, *Phys. Rev. B* **58**, 16221 (1998).
- [29] [See Supplementary Material, that includes Refs. \[43–46\]](#).
- [30] H. J. Krenner, S. Stuffer, M. Sabathil, E. C. Clark, P. Ester, M. Bichler, G. Abstreiter, J. J. Finley, and A. Zrenner, *N. J. Phys.* **7**, 184 (2005).
- [31] M. F. Doty, J. I. Climente, A. Greulich, M. Yakes, A. S. Bracker, and D. Gammon, *Phys. Rev. B* **81**, 035308 (2010).
- [32] M. A. Migliorato, A. G. Cullis, M. Fearn, and J. H. Jefferson, *Phys. Rev. B* **65**, 115316 (2002).
- [33] V. Jovanov, T. Eissfeller, S. Kapfinger, E. C. Clark, F. Klotz, M. Bichler, J. G. Keizer, P. M. Koenraad, M. S. Brandt, G. Abstreiter, and J. J. Finley, *Phys. Rev. B* **85**, 165433 (2012).
- [34] G. L. Bir, G. E. Pikus, P. Shelnitz, and D. Louvish, *Symmetry and strain-induced effects in semiconductors* (Wiley New York, 1974).
- [35] C. Pryor, *Phys. Rev. B* **57**, 7190 (1998).
- [36] G. Bester, X. Wu, D. Vanderbilt, and A. Zunger, *Phys. Rev. Lett.* **96**, 187602 (2006).
- [37] S. Schulz, M. A. Caro, E. P. O'Reilly, and O. Marquardt, *Phys. Rev. B* **84**, 125312 (2011).
- [38] G. Tse, J. Pal, U. Monteverde, R. Garg, V. Haxha, M. A. Migliorato, and S. Tomić, *J. Appl. Phys.* **114**, 073515 (2013).
- [39] K. Gawarecki, P. Machnikowski, and T. Kuhn, *Phys. Rev. B* **90**, 085437 (2014).
- [40] M. Zieliński, Y. Don, and D. Gershoni, *Phys. Rev. B* **91**, 085403 (2015).
- [41] G. Bester and A. Zunger, *Phys. Rev. B* **71**, 045318 (2005).
- [42] M. Usman, Y. H. M. Tan, H. Ryu, S. S. Ahmed, H. J. Krenner, T. B. Boykin, and G. Klimeck, *Nanotechnology* **22**, 315709 (2011).
- [43] K. Müller, A. Bechtold, C. Ruppert, T. Kaldewey, M. Zecherle, J. Wildmann, M. Bichler, H. Krenner, J. Villas-Bôas, G. Abstreiter, and J. Finley, *Ann. Phys.* **525**, 49 (2013).
- [44] B. A. Foreman, *Phys. Rev. B* **48**, 4964 (1993).
- [45] M. Świdorski and M. Zieliński, *Acta Phys. Pol. A*, *in press* (2015).
- [46] C. Pryor, J. Kim, L. W. Wang, A. J. Williamson, and A. Zunger, *J. Appl. Phys.* **83**, 2548 (1998).